Chapter 3: Data Acquisition and Processing

The data acquisition includes the optical system, control software, data storage, and initial processing.

3.1 Spectrometer

The spectrometer used was produced by Ocean Optics, model USB-650. It has a wavelength range of 349nm to 999nm, with a resolution of 2nm (FWHM). It has 651 pixels and an adjustable integration time from 3ms to 65s.

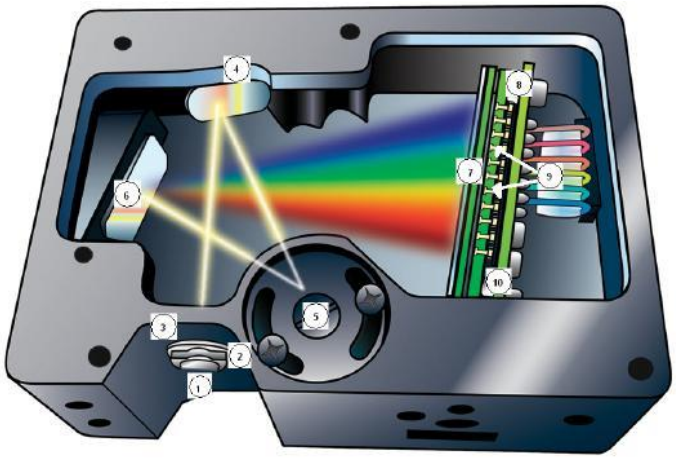

Figure 3.1: USB-650 internal view from manual [6]

3.2 Optical System

The Helimak plasma was viewed through an optical port on the bottom of the machine as seen in figure 3.2. The physical window was approximately 40cm wide, and gives a maximum effective viewing range of about 35cm for a 50mm lens. The lens was mounted on a ruled linear track which also served as a position measurement. The lens was connected to the spectrometer through an optical fiber of approximately 2m in length.

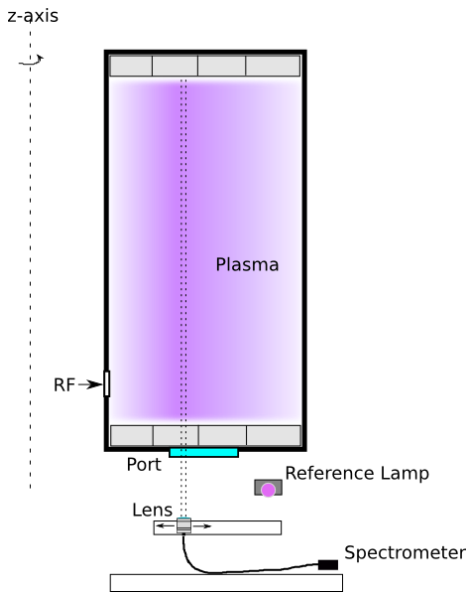

Figure 3.2: Optical system layout

The starting position of the track was measured from the inner radius of the Helimak chamber using a plumb line from the chamber to the track's position. The inner radius of the chamber was also measured to give the starting radius of the track. There were two track segments. The starting radius of the second track was also measured relative to the first track.

3.3 Lens, Fiber, and Spectrometer Calibration

Calibration of the combination of the lens, fiber optic, and the spectrometer where done by taking the setup and measuring a known calibrated lamp, which has performed by William Rowan using a Lab-Sphere source at MIT. The known spectral radiance profile of the lamp $L(\lambda)$, given in units of $[\frac{W}{cm^2 \times sr \times nm}]$, was used to calculate a calibration constant $K(\lambda)$. A measurement of the lab-sphere emissions was made using the combination of lens, optical fiber, and spectrometer. The calibration

constant was then determined using eq. 3.1, where $N(\lambda)$ is the number of counts at a given wavelength with background subtracted, and $L(\lambda)$ is the known radiance of the lamp at that wavelength, and Δt is the integration time used for the measurement. The constant can then be used to calculate the radiance of the plasma from the number of counts on the spectrometer for later measurements. The determined calibration is shown in figure 3.3.

$$K(\lambda) = \frac{N(\lambda)}{\Delta t\, L(\lambda)} \tag{3.1}$$

$$L(\lambda) = \frac{N(\lambda)}{\Delta t\, K(\lambda)} \tag{3.2}$$

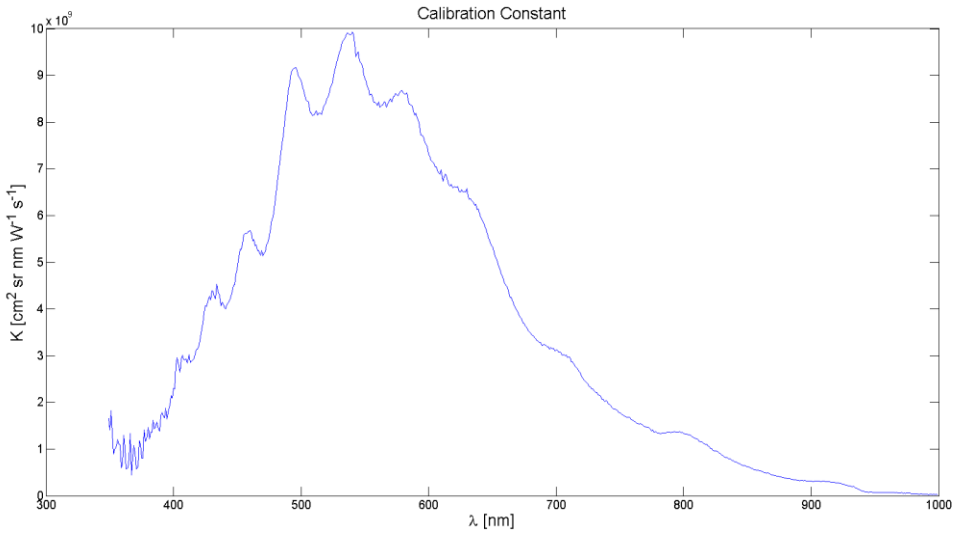

Figure 3.3: Calibration constant K versus wavelength

3.4 WINDOW CALIBRATION

The optical transmission qualities of the port window where measured as a function of position along the width of the window to account for any variations. The window also has a copper mesh screen on top of it to prevent RF power from escaping through the port. Calibration was accomplished by removing the entire window and screen and mounting in on a linear track. A reference light source was positioned on one side and the lens on the other, as seen in figure 3.4.

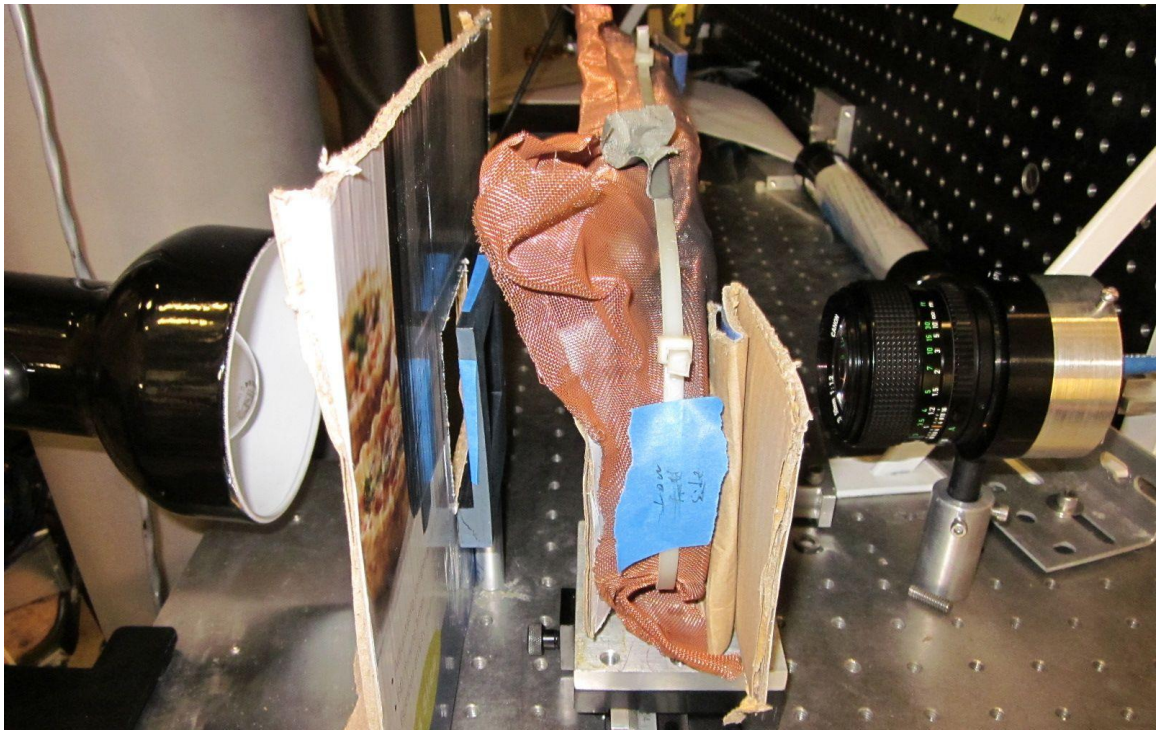

Figure 3.4: Window calibration setup

The reference light source consisted of a standard light bulb and a diffusor made a piece of paper. A measurement of the light source was made without the window in place to serve as a reference, as well as a background reference. The cardboard served to block

light to prevent the light from reflecting off of other surfaces which might contribute to the measurements.

Transmission measurements were made at 1cm increments along the length of the window. At each position, several spectra was taken and averaged together. The transmission of the window versus wavelength was calculated by dividing the measurements at each position by the measurement made without the window in place with background subtracted. That is, the transmission is $C(\lambda, x) = I(\lambda, x)/I_0(\lambda)$. A sample of the transmission profile versus wavelength can be seen in figure 3.5 measured at position of 15cm from high field side. Figure 3.6 shows average transmission over all wavelengths versus position.

This transmission factor was included in the calibration constant for the lens/fiber/spectrometer by defining a total calibration constant in eq. 3.3.

$$K_{tot}(\lambda, x) = C(\lambda, x)K(\lambda) \tag{3.3}$$

The total calibration constant could then be used as the absolute calibration of the optical system when the lens is then aimed through the same window after it was mounted back on the Helimak. This does not, however, account for any reflections from the opposite side of the vacuum chamber as there is no proper optical dump there to prevent scattered light from entering the optics. This could cause the system to over-estimate the emission of the plasma.

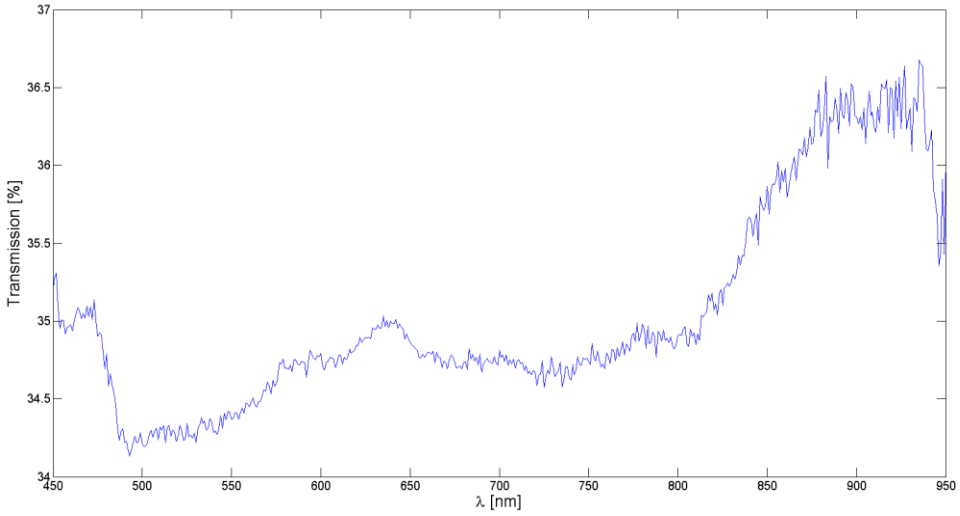

Figure 3.5: Window transmission versus wavelength at x=15cm

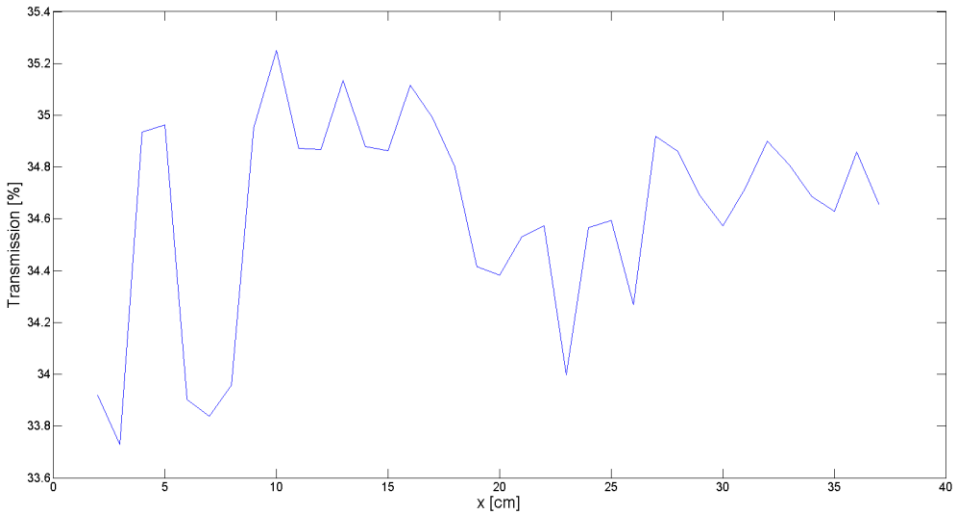

Figure 3.6: Average window transmission versus position

3.5 NEUTRAL GAS PRESSURE ACQUISITION

The neutral gas pressure was obtained from a hot filament ionization gauge which is located near the pumping system. The ionization gauge controller had a voltage output for automatic recording of the pressure. The pressure decade, in units of Torr, was given by the most significant voltage unit, and the linear scale was given by the lower significant units.

The raw voltage output was recorded by one channel of a National Instruments USB-6008 multifunction DAQ as in figure 3.7. The acquisition Labview vi recorded the conversion to pressure in Torr as well as recorded the raw voltage. Only pressure readings right before each shot was taken to avoid interference from the shot itself when the data was analyzed.

Ionization gauges are typically calibrated for measuring pressure in Nitrogen, but will measure higher or lower when measuring other gases. A correction factor must be applied to the pressure reading for other gases. For Argon this factor is 1.29[7]. The actual pressure is then determined by dividing the recorded pressure by this correction factor.

Figure 3.7: USB-6008 used acquire voltage output from ionization gauge controller.

3.6 SPECTRAL ACQUISITION

A Labview vi was written to control and acquire data from the USB-650 spectrometer using the Ocean Optics Labview interface library. The control panel can be seen in figure 3.8. The vi allowed similar controls to the standard Ocean Optics control software, but also allowed customized actions.

The vi connected to the MDSPlus database of the Helimak control system, and used the MDSPlus shot event that is sent out at the beginning of each shot to automatically synchronize data acquisition with the shot. The signal was received several seconds before the shot began, which allowed acquisition during the entire shot that lasts approximately 30s.

The control panel allowed the user to set multiple integration times for the spectrometer to use during the shot. Each integration time was used in sequential order. After it had used one of each integration time it would start again with the first one. This allowed for frames with long integration times to be used for parts of the spectrum which are not as bright as other parts, while the shorter integration times are used for the intense parts of the spectrum which would saturate the detector for the longer integration times.

The control panel also had input fields for data related to the optical system, such as which lens and fiber were being used, the location and orientation of the lens during the shot, or other information that could be useful at a later date in analyzing the spectra. Once it finished acquiring the spectra during the shot, it would store the data in a human readable text file as. The user would then have to set it to start waiting for the next shot.

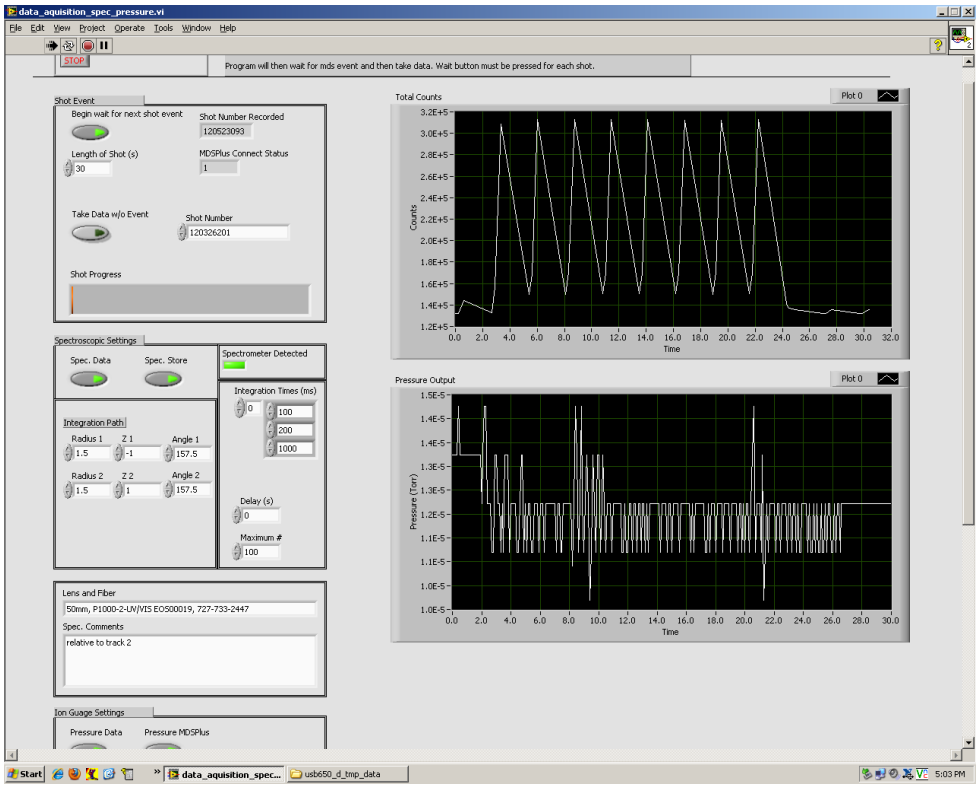

Figure 3.8: Labview acquisition control panel

In the sample screen-shot of the vi is shown in figure 3.8 there are two plots shown on the right of the control panel to summarize the results at the end of each shot. The top plot shows the total number of counts from the spectrometer summed over all wavelengths versus time. The saw-tooth pattern is a result of sequentially longer and shorter integration times. Longer integrations have more counts. The start and end of plasma formation can be seen from this plot.

The bottom plot gives the recorded pressure from the ionization gauge during the shot. Some variation of the pressure reading was observed during shots, but it is not known if this is a real pressure change or if the ionization gauge was affected by the Helimak's magnetic field or some other effect during the shot.

3.7 DATA STORAGE

After each shot the vi would write the data to a data file which had a similar structure the data would have in MDSPlus. The first line of each data segment in the file contained the MDSPlus node name the data should be put into. The second line contained the data type; either numeric=0 or string=1. The third line contained the number of dimensions of the data: either 1D or 2D. If 1D then the fourth line gave the number of lines of data before the next data entry and the fourth line starts listing the data. If 2D then the third line gives the number of lines and the fourth line gives the number of columns.

The vi would also write to a status file which contained a number representing the status of data collection. A '0' in the file meant that collection is waiting for a shot. A '-1' in the file means data collection has ended and is not waiting for any more shots. Otherwise the number in the file was equal to the shot number from which new data was collected. A script running in IDL would wait until the status file contained a new shot number, and would load the data from the corresponding data file into MDSPlus. The script would terminate when the status was set to '-1'.

MDSPlus does has a Labview interface which would have allowed the vi to load the data directly, but the interface was found to give unpredictable results. Also, the data file acted as a human readable backup of the data.

3.8 PROCESSING RAW DATA

Before the data is used to perform analysis, initial processing was done to average all the spectra of the same integration time, apply the calibration, and to convert the raw spectra into population densities of excited states for both neutral and singly ionized Argon. A sample spectrum with an integration time of 200ms is given in figure 3.9 after averaging over all the raw spectrum of the same integration time and subtracting the

background. Figure 3.10 shows the spectrum after absolute radiance calibration is applied.

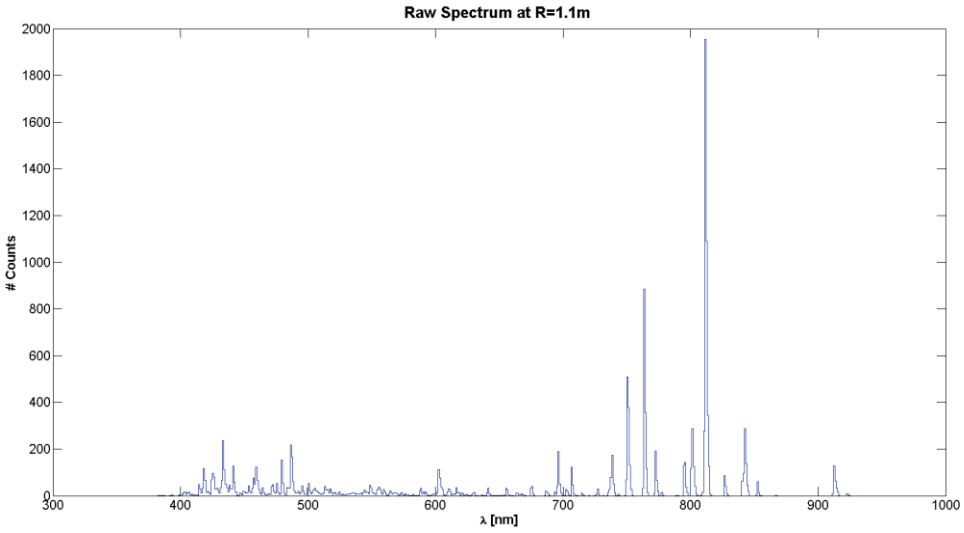

Figure 3.9: Raw spectrum at absolute radial position of 1.1m, near the peak of the temperature and density of the Helimak with an integration of 200ms.

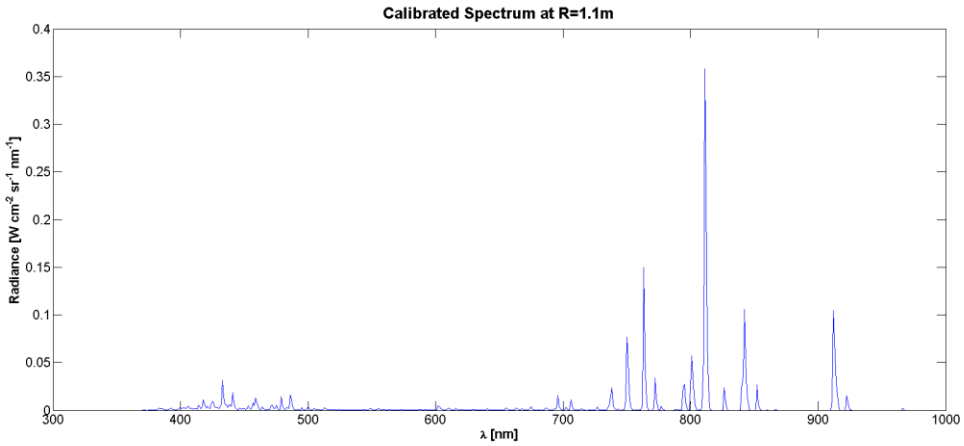

Figure 3.10: Calibration of the raw spectrum in figure 3.9 gives absolute radiance of light coming from Helimak plasma.

The lines below about 500nm are coming from singly ionized Argon, while the lines about 700nm come from neutral Argon. Several Hydrogen lines can also be seen between the two groups, perhaps from some residual water vapor in the vacuum chamber. When the integration time of 1000ms was used as in figure 3.11, some of the dimmer lines become more defined. However, the stronger lines have saturated the spectrometer, and the values of radiance for those lines are not correct.

The next step was to convert the spectrum into population densities for the excited states of interest. Conceptually this involves integrating over a single line to get the total radiance of that line. The total radiance is related to the emission from the plasma by a chord integral representing a narrow cone from the collection lens extending through the plasma: $L_{tot} = \frac{hc}{\lambda}\int_0^l dl'\epsilon$, where ϵ is the angular photon number emission density from a single transition in $[s^{-1}sr^{-1}cm^{-3}]$. However, since the plasma should be nearly uniform in the vertical direction, the emission density should be nearly a constant. The integral would then simply be the length of the cord l multiplied by the emission density ϵ.

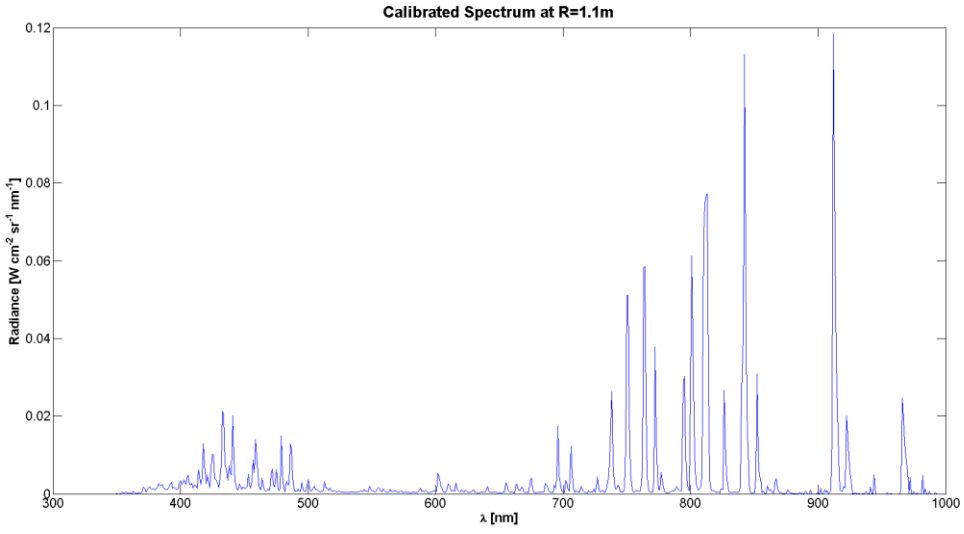

Figure 3.11: Calibrated spectrum at same radial position as figure 3.10, but with an integration time of 1000ms.

The Einstein coefficient for the transition of interest A_{ji} gives the effective frequency in $[s^{-1}]$ for the transition from excited state j to state i. It is assume the emission is isotropic which gives the emission density in terms of the population density of upper state j: $\epsilon = \frac{1}{4\pi} A_{ji} n_j$. Within the collisional-radiative models the micro states are grouped into a common state. The population density of each microstate is found in terms of the modeled state through the fractional statistical weight: $n_j = \frac{g_j}{g_k} n_k$, where $g_k = \sum g_j$ is the sum is over all microstates of state k. The population density of one of the modeled excited states can then be written in terms of the absolute radiance L_{tot} as measured from the plasma and the chord integral through the plasma of length l as in eq. 3.4.

$$n_k = \frac{g_k}{g_j} \frac{4\pi L_{tot}}{l A_{ji}} \frac{\lambda}{hc} \tag{3.4}$$

3.9 Atomic Levels and Transitions

For neutral Argon, the upper state density is calculated for four different states that are modeled [4]. For singly ionized Argon, it is calculated for three upper states.

For some upper states multiple transitions, or lines, are used in the determination of the density. Only those lines which do not ambiguously overlap with lines of other levels are used, which reduced the total number of available lines. If two lines from the same model level do overlap, both are used with the Einstein coefficients weighted by the statistical weights of the microstates. A total of sixteen lines are used.

line	$\lambda\ [nm]$	Ion	Upper State	Model #	$\frac{g_j}{g_k}\frac{hc\,A_{ji}}{4\pi\lambda}\ [Wsr^{-1}]$	Δt [ms]
1	434	Ar II		14	2.123e-12	1000
2	442.8	Ar II		14	1.282e-12	1000
3	480.6	Ar II		13	1.283e-12	1000
4	487.98	Ar II		15	1.600e-12	1000
5	696.5431	Ar I	$^2P_{1/2}4p[1/2]_1$	9	1.451e-13	1000
6	706.7218	Ar I		8	5.315e-14	1000
7	738.398	Ar I		8	1.134e-13	1000
8	763.5106	Ar I		7	1.268e-13	200
9	794.8176	Ar I		8	1.388e-13	1000
10	801	Ar I		7	6.999e-14	1000
11	811	Ar I		7	2.990e-13	200
12	826.4522	Ar I		9	2.928e-13	1000
13	852.1442	Ar I		8	9.675e-14	1000
14	912.2967	Ar I		6	3.277e-13	200
15	922.4499	Ar I		7	2.156e-14	1000
16	965.7786	Ar I		6	8.893e-14	1000

Table 3.1: Data used to convert the measured lines to population densities relating to the available models. One model for the Ar I levels, and one for the Ar II levels. Δt is the integration time used for each line.